Geophys. J. Int. (2006) **166,** 991–998 doi: 10.1111/j.1365-246X.2006.03061.x

Geodetic observations of ice flow velocities over the southern part of subglacial Lake Vostok, Antarctica, and their glaciological implications

Jens Wendt,[1,2] Reinhard Dietrich,[1] Mathias Fritsche,[1] Anja Wendt,[1,2] Alexander Yuskevich,[3] Andrey Kokhanov,[3] Anton Senatorov,[3] Valery Lukin,[4] Kazuo Shibuya[5] and Koichiro Doi[5]

[1]*Dresden University of Technology, Institut für Planetare Geodäsie,* 01062 *Dresden, Germany. E-mail: jwendt@cecs.cl*
[2]*Centro de Estudios Científicos, Av. Arturo Prat* 514, *Valdivia, Chile*
[3]*Aerogeodeziya, ul. Bukharestskaya* 8, 192102 *St. Petersburg, Russia*
[4]*Arctic and Antarctic Research Institute, Russian Antarctic Expedition, ul. Beringa* 38, 199397 *St. Petersburg, Russia*
[5]*National Institute of Polar Research, Polar Research Resources Center, Kaga* 1-19-10, *Itabashi-ku, Tokyo* 173-8515, *Japan*

Accepted 2006 May 5. Received 2006 April 27; in original form 2005 November 23

SUMMARY

In the austral summer seasons 2001/02 and 2002/03, Global Positioning System (GPS) data were collected in the vicinity of Vostok Station to determine ice flow velocities over Lake Vostok. Ten GPS sites are located within a radius of 30 km around Vostok Station on floating ice as well as on grounded ice to the east and to the west of the lake. Additionally, a local deformation network around the ice core drilling site 5G-1 was installed.

The derived ice flow velocity for Vostok Station is $2.00\,\mathrm{m\,a^{-1}} \pm 0.01\,\mathrm{m\,a^{-1}}$. Along the flowline of Vostok Station an extension rate of about $10^{-5}\,\mathrm{a^{-1}}$ (equivalent to $1\,\mathrm{cm\,km^{-1}\,a^{-1}}$) was determined. This significant velocity gradient results in a new estimate of 28 700 years for the transit time of an ice particle along the Vostok flowline from the bedrock ridge in the southwest of the lake to the eastern shoreline. With these lower velocities compared to earlier studies and, hence, larger transit times the basal accretion rate is estimated to be $4\,\mathrm{mm\,a^{-1}}$ along a portion of the Vostok flowline. An assessment of the local accretion rate at Vostok Station using the observed geodetic quantities yields an accretion rate in the same order of magnitude. Furthermore, the comparison of our geodetic observations with results inferred from ice-penetrating radar data indicates that the ice flow may not have changed significantly for several thousand years.

Key words: Antarctica, geodesy, glaciology, GPS, ice flow velocity, Lake Vostok.

1 INTRODUCTION

Lake Vostok, the largest of about 150 known subglacial lakes in Antarctica (Siegert *et al.* 2005), is more than 250 km long. It is covered by an ice sheet about 4000 m thick and has a depth of up to 1200 m (Kapitsa *et al.* 1996; Masolov *et al.* 2001; Studinger *et al.* 2003). In recent years, this lake attracted remarkable scientific as well as public attention, because of its potential to harbour ancient life isolated by the thick ice sheet. The evidence of first microbes in the lowermost part of the Vostok ice core, which consists of ice accreted to the bottom of the ice sheet has excited scientific controversy (Karl *et al.* 1999; Priscu *et al.* 1999; Bulat *et al.* 2004).

Furthermore, the lake itself is of geoscientific interest. It has been suggested that some subglacial lakes are located near the onset of enhanced ice-flow features (Siegert & Bamber 2000) which drain a substantial part of the ice sheet. Recently, lake level variations of subglacial lakes in the Adventure Subglacial Trench, East Antarctica, were detected (Wingham *et al.* 2006) indicating the rapid discharge of one lake into the others.

To understand how the largest subglacial lake influences the general ice flow, both modelling (Mayer & Siegert 2000; Pattyn *et al.* 2004) and observations are indispensable. In addition to the determination of the magnitude of the ice flow velocity, its spatial distribution is important to draw conclusions on the transit time of the ice across the lake. Strain parameters, derived from the velocities, are essential for the interpretation of the 3600 m long ice core which represents a unique climate record (Petit *et al.* 1999). Moreover, they can be used to assess the mass balance of the ice in that area.

2 OBSERVATIONS

During the austral summer seasons 2001/2002 and 2002/2003 extensive GPS measurements were performed in the vicinity of the

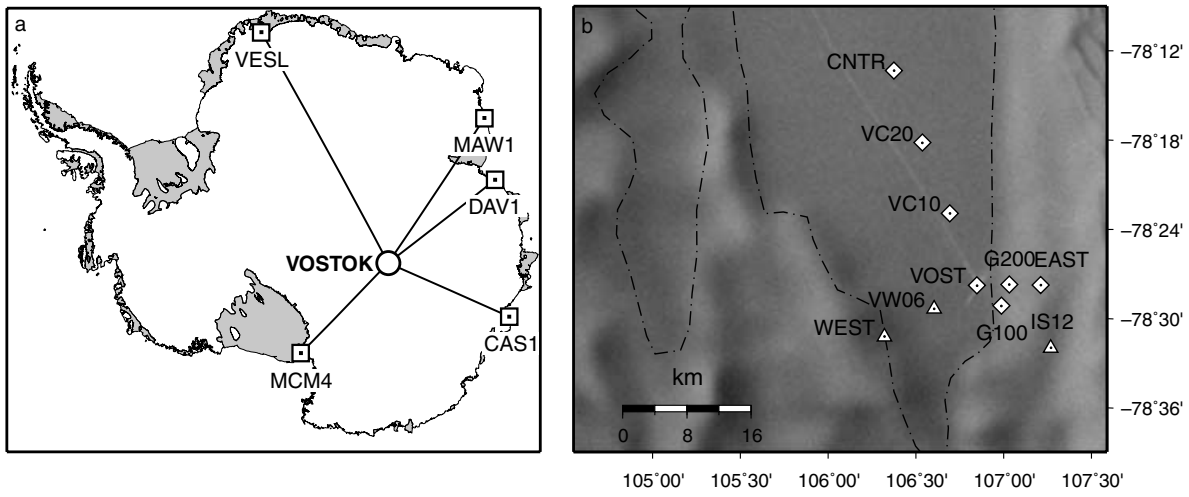

Figure 1. GPS sites in the Lake Vostok area. (a) Baselines between the permanent GPS stations Sanae IV (VESL), Mawson (MAW1), Davis (DAV1), Casey (CAS1), and Mc Murdo (MCM4) and the temporary GPS sites in the vicinity of Vostok Station. (b) GPS sites in the south of Lake Vostok. Sites marked by diamonds were occupied in 2001/2002 and 2002/2003; triangles indicate sites that were only observed during 2002/2003. The map is oriented north up, background: Radarsat mosaic (Jezek & RAMP Product Team 2002), lake boundary: Bell *et al.* (2002).

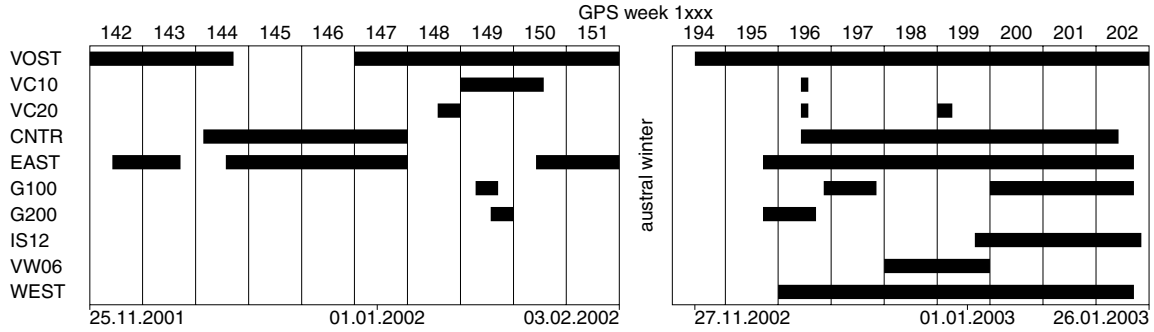

Figure 2. Observation schedule during the austral summer seasons 2001/02 (left) and 2002/03 (right). GPS measurements were carried out at a total of ten locations. Site occupations are displayed by black bars.

Russian Antarctic research station Vostok (Fig. 1). Network and observation schedule (Fig. 2) were designed for the precise determination of the horizontal ice flow in this area and for investigating height changes of the surface above Lake Vostok as a response to tidal and atmospheric pressure forcing (Wendt *et al.* 2005). During the first season, seven GPS sites (VOST, EAST, CNTR, VC10, VC20, G100 and G200) were installed over the southern part of subglacial Lake Vostok and the adjacent eastern area (Table 1). An additional three sites (WEST, VW06, IS12) were established one year later to extend the area under investigation to the west and to the south (Fig. 1).

Each site consists of one central mark and two reference marks represented by wooden stakes with a diameter of 6 cm, a total length of 80 cm and a height above the snow surface of about 30 cm. The use of such relatively short stakes is feasible because of the low snow accumulation rate in the area of only about 6 cm a^{-1} (Barkov & Lipenkov 1996) and improves the stability of the marks. During site occupation the GPS antenna was mounted on a forced centring device incorporated into the top of the central stake. The reference marks served as a stability check of the central mark using tape measurements and geometric levelling. The intercomparison of these measurements in both seasons showed a consistency better than 1 cm for the side lengths of the triangles and of about 1 mm for the height differences. Geodetic dual frequency receivers Trimble 4000 SSi together with microcentred antennas with ground plate (`TRM33429.00+GP`) were used for the GPS observations.

Table 1. Ellipsoidal coordinates of the GPS sites (Ellipsoid: GRS80).

	Latitude [° South]	Longitude [° East]	Height [m]
VOST	78.47	106.83	3478
VC10	78.39	106.68	3483
VC20	78.31	106.52	3488
CNTR	78.23	106.36	3491
EAST	78.46	107.19	3471
G100	78.49	106.97	3478
G200	78.49	107.01	3479
IS12	78.53	107.25	3463
VW06	78.49	106.59	3475
WEST	78.52	106.32	3469

In addition to the GPS sites described so far, a local deformation network consisting of six sites within a radius of 1.25 km from the drilling site 5G-1 (close to VOST) was installed. This network was observed during both field seasons using differential GPS relative to the local reference station VOST.

3 DATA ANALYSIS AND RESULTS

The processing of the GPS data was performed using the BERNESE GPS SOFTWARE 5.0 (Hugentobler *et al.* 2004). We applied identical standard procedures to the data sets of both seasons including precise orbits and earth rotation parameters provided by the International GNSS Service (IGS).

The connection to the terrestrial reference frame was established by computing baselines to permanent tracking stations of the IGS close to the Antarctic coast (Fig. 1a). For these stations, site coordinates and velocities according to IGb00 (Ray *et al.* 2004; IGb00 2004) were introduced. This reference frame is a consistent GPS realization of the International Terrestrial Reference Frame ITRF2000 (Altamimi *et al.* 2002; Boucher *et al.* 2004) possessing the identical geodetic datum.

Daily positions for the GPS sites in the Vostok area obtained from this analysis form the basis of the following investigations. To estimate the flow velocities, the daily normal equations were solved for the unknown site coordinates and velocities. These parameters refer to the same earth-fixed reference frame as the reference sites represented by the realization IGb00. Therefore, the plate motion of the Antarctic Plate—a clockwise rotation around the Euler pole at 63.0°S, 234.7°E (Dietrich *et al.* 2004)—has to be accounted for in order to obtain the ice surface velocities relative to bedrock. For Vostok Station the plate motion results in a displacement rate of 12 mm a^{-1} with an azimuth of 194.7°. Fig. 3 gives a close-up view on the trajectories of daily horizontal positions for the sites CNTR, EAST and VOST. These sites were occupied for several weeks in both field seasons (see Fig. 2). The alignment of the individual daily solutions to the final rates gives a first impression of the high precision of the estimates.

To answer the question of how long an observation period is needed to achieve a reliable velocity estimate, the number of observation days in the velocity estimation was successively increased. The convergence of the flow velocity determination based on these daily positions as a function of observation period is shown in Fig. 4 for the sites CNTR, EAST, VOST and WEST in the second season.

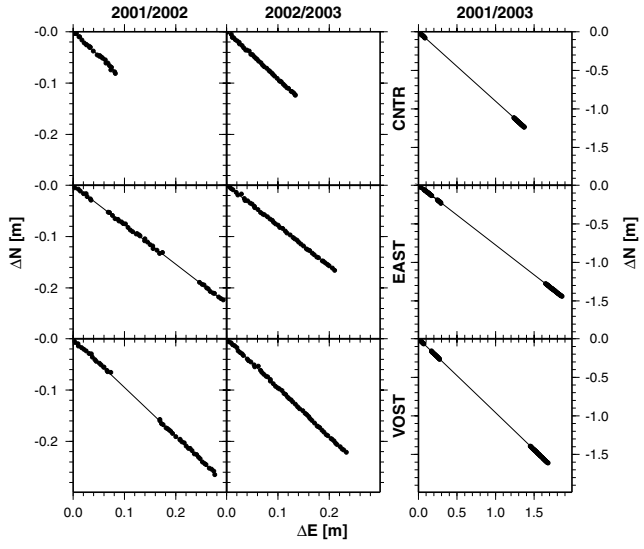

Figure 3. Daily positions (north and east components) relative to the initial positions for the stations CNTR, EAST and VOST. Each field season is displayed separately and can be compared with the entire observation period (right hand column) covering the interval from November 2001 to January 2003 (*cf.* Fig. 2).

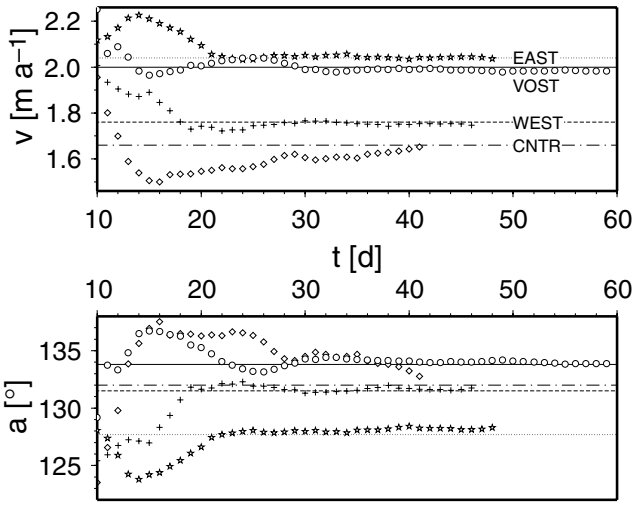

Figure 4. Convergence of the estimates of the horizontal flow velocity v and the azimuth a as a function of the observation period t for the sites CNTR, EAST, VOST, and WEST during field season 2002/03. Final results (Table 2) are drawn as horizontal lines.

After 30–40 days the solution for the magnitude agrees with the final one within the one-sigma limits. However, the accuracy of the determined direction also depends on the absolute displacement within the observed time span and, therefore, it can take longer to reach a stable solution.

The final estimates of horizontal and vertical ice flow velocities with respect to the Antarctic Plate and their accuracies based on all available data are summarized in Table 2. The estimates of the two field seasons are consistent with the results for the whole period demonstrating the reliability of the final solution. It also confirms—as expected—the hypothesis of a constant flow rate throughout the year. The derived horizontal ice flow velocities have an accuracy of 10 mm a^{-1} (one sigma level) for all sites which were observed during both field seasons. The final vectors of horizontal ice flow are shown in Fig. 5.

Due to the satellite constellation of GPS, vertical velocities are usually less precise than the horizontal ones. Another factor complicating the estimation of a mean vertical velocity of sites on the lake surface is a higher variability of the vertical position due to the response of the lake to tidal and atmospheric forcings (Wendt *et al.* 2005). These effects can cause up to ±20 mm elevation changes within days and weeks. This characteristic and the small magnitude

Table 2. Horizontal ice flow velocities v, azimuths a (relative to true north), and vertical ice-particle velocities w together with their standard deviations s_v, s_a, s_w. Estimates are based on the combination of two field seasons except for GPS sites marked by * (see Fig. 2).

Site	v [m a^{-1}]	s_v [m a^{-1}]	a [°]	s_a [°]	w [m a^{-1}]	s_w [m a^{-1}]
CNTR	1.66	0.01	131.8	0.3	−0.06	0.02
VC20	1.80	0.01	132.4	0.3	−0.06	0.02
VC10	1.92	0.01	133.7	0.3	−0.06	0.02
VOST	2.00	0.01	133.7	0.3	−0.07	0.02
G100	2.03	0.01	132.3	0.3	−0.06	0.02
G200	2.02	0.01	131.5	0.3	−0.05	0.02
EAST	2.04	0.01	127.6	0.3	−0.06	0.02
IS12*	2.05	0.05	128.9	1.3		
VW06*	1.94	0.09	135.1	2.6		
WEST*	1.76	0.02	131.1	0.5		

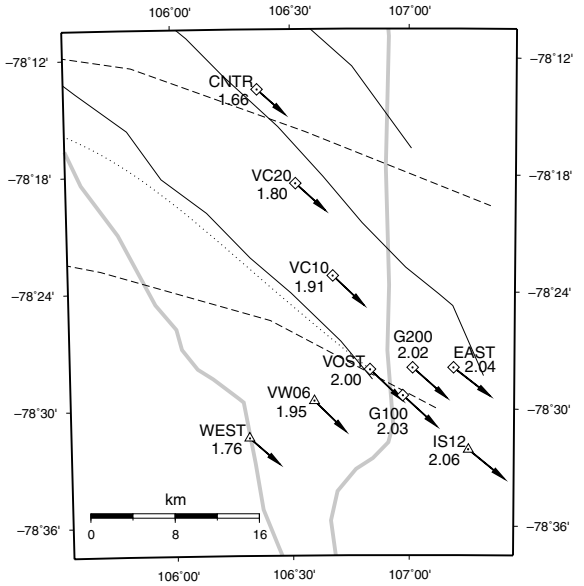

Figure 5. Comparison of ice flow directions derived from different techniques. Black vectors: GPS-derived ice flow directions (this study), full black lines: results of structure tracking over Lake Vostok (Bell *et al.* 2002), dashed black lines: trajectories based on InSAR (Kwok *et al.* 2000), dotted black line: computed flowline along the maximum-slope direction of the surface elevation (Parrenin *et al.* 2004), grey line: lake boundary.

of the vertical motion inhibit a precise determination of the vertical velocity within one season. However, as tidal and air pressure effects are stationary processes without long-term trends, observations of both seasons yield a reliable estimate for the vertical velocity.

4 INTERPRETATION

4.1 Horizontal velocity field and comparison with earlier studies

For Vostok Station the ice flow velocity has been determined previously by astronomical positioning (Liebert & Leonhardt 1973), SAR interferometry (Kwok *et al.* 2000) and earlier GPS measurements (Bell *et al.* 2002). Given the error margins a comparison of these earlier results with the present investigation (Table 3) shows that the flow velocity at Vostok Station has previously been overestimated. However, the estimates of the flow direction for this site agree within about 10°.

The GPS results (Fig. 5) reveal a general increase in velocity from the northwest to the southeast and thus indicate a significant acceleration of the ice during its transit across the lake.

It is interesting to note that this increase of horizontal velocity observed for the southernmost part of Lake Vostok differs from model results. For a flowline farther north in the central part of the lake, a 2-D isothermal model predicts an almost constant velocity across the lake (Mayer & Siegert 2000). A 3-D time-dependent thermomechanical ice sheet model including higher-order stress gradients yields an acceleration as the ice enters the lake and, especially in the north, a subsequent decrease in velocity towards the eastern margin (Pattyn *et al.* 2004). For our section of the velocity field the observed pattern is different from both models.

Table 3. Comparison of the observed horizontal ice flow velocity for Vostok Station.

Observation technique	v [m a^{-1}]	s_v [m a^{-1}]	a [°]	s_a [°]	Source
astrogeod.	3.7	0.7	142	10	Liebert & Leonhardt (1973)
InSAR	4.2	0.3	130	N/A	Kwok *et al.* (2000)
GPS	3.0	0.8	131	4	Bell *et al.* (2002)
GPS	2.00	0.01	133.7	0.3	This study

A differential velocity field (Fig. 6a) is derived by subtracting the vector of site CNTR from all other velocity vectors. This GPS site can be employed without loss of precision as a reference point because its velocity vector is based on the combination of both field seasons. Thus, its estimate is one of the most precise and reliable ones (Fig. 3 and Table 2). The differential velocity field emphasizes the general change in velocity from the northwest to the southeast. In addition to the acceleration across the lake, it also illustrates a divergent flow in the vicinity of Vostok Station and an eastward deflection of the flowlines close to and beyond the southeastern shoreline.

The flow direction at the GPS sites can also be compared with earlier determinations (Fig. 5). The long-term flow trajectories determined by structure tracking in successive east–west ice-penetrating radar profiles (Bell *et al.* 2002; Tikku *et al.* 2004) are in good agreement with the flow directions obtained by GPS. Thus, the current surface flow directions derived from one year of observations agree with the ones of deeper layers representing the flow directions since this ice entered the lake.

In contrast, the ice flow directions according to the velocity field derived from SAR interferometry (Kwok *et al.* 2000) show larger deviations which may reflect specific problems in applying InSAR in this context. In particular, the unfavourable error propagation due to the relative geometry of ascending and descending satellite tracks and the large distance to the point of assumed zero velocity on Ridge B might have increased the uncertainties. Vertical movements of the lake surface (Wendt *et al.* 2005), which overlay the horizontal displacement signal in the InSAR fringe pattern, were not considered at all. Therefore, the obtained flow pattern over the lake area might be affected in a systematic way.

Finally, a computed flowline (Parrenin *et al.* 2004) based on the surface gradient derived from an accurate Digital Elevation Model (DEM) of the Antarctic ice sheet (Rémy *et al.* 1999) coincides well with the observed ice flow direction.

4.2 Strain analysis

The measured position changes of the GPS sites reflect the deformation process of the ice sheet during the observation period. These quantities were employed to estimate the deformation parameters applying the theory of infinitesimal homogeneous strain (Hooke 1998) and assuming steady state flow of the ice sheet which implies constant flow rates. To calculate the strain parameters, the area around Vostok Station was subdivided into finite elements defined by the site geometry (Fig. 6). Two kinds of elements can be distinguished: six equilateral triangles with 1.25 km side length within a local deformation network designed for a strain analysis and elements connecting those regional GPS sites which provide a suitable geometry for this analysis.

The deformation tensor of the individual cells was split up into a symmetric part (the strain tensor) and the antisymmetric part expressing the differential network rotation. An eigenvalue decomposition of the strain tensor reveals the principal strain rates $\dot{\epsilon}_{\max}$ and $\dot{\epsilon}_{\min}$ as well as the principal direction Θ of $\dot{\epsilon}_{\max}$.

Both the local deformation network and the network of remote stations (G100, G200, VW06, VC10, see Fig. 6b) clearly indicate

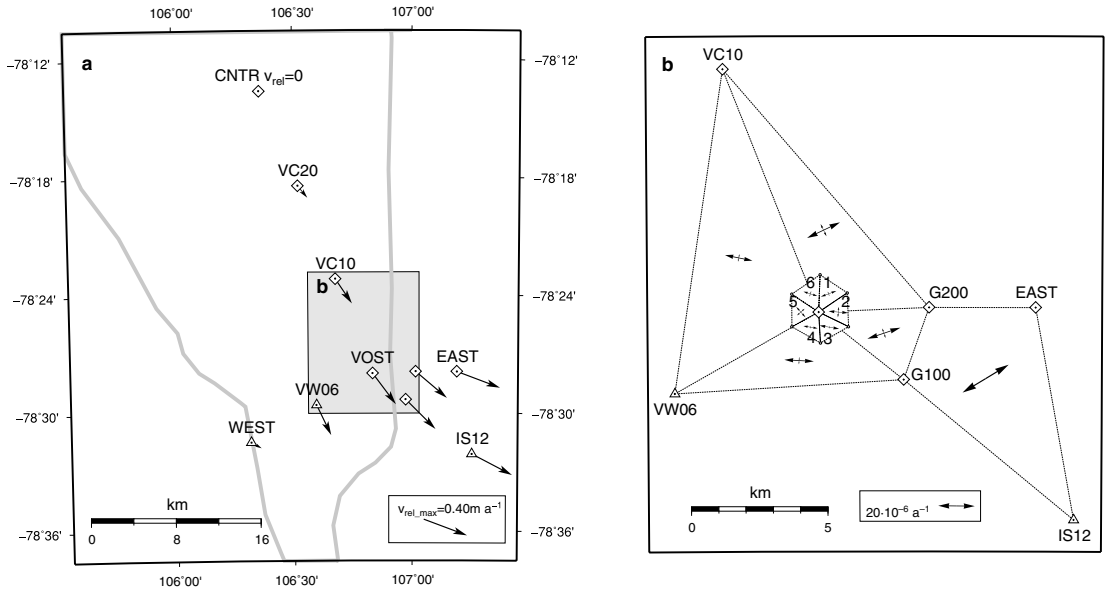

Figure 6. (a) Relative velocity field with respect to CNTR (differential vectors), grey line: lake boundary. (b) Surface strain rate principal axes in the vicinity of Vostok Station.

Table 4. Horizontal strain rates $\dot{\epsilon}$, their principal directions Θ relative to true north with respect to a fixed Antarctic Plate, and the corresponding standard deviations s derived from the GPS measurements (*cf.* Fig. 6).

Finite element	$\dot{\epsilon}_{\max}$ [10^{-6} a^{-1}]	$s_{\dot{\epsilon}_{\max}}$	$\dot{\epsilon}_{\min}$ [10^{-6} a^{-1}]	$s_{\dot{\epsilon}_{\min}}$	Θ [°]	s_Θ [°]
Local deformation network 5G-1						
1	9.1	2.3	2.6	2.1	69.2	13.9
2	10.6	2.3	5.8	2.3	94.6	19.2
3	10.7	2.3	1.6	2.5	99.4	10.7
4	7.9	2.4	1.8	2.5	99.1	16.3
5	7.6	2.3	5.5	2.5	138.5	46.6
6	7.8	2.4	3.3	2.0	107.3	20.1
mean	8.6	0.80	3.9	0.77	95.1	6.7
VOST–G100–G200	19.1	3.9	5.4	4.5	71.1	12.5
VOST–VC10–G200	19.9	4.0	7.4	1.3	64.4	9.6
VOST–VC10–VW06	15.2	2.6	4.2	1.2	101.3	7.4
VOST–G100–VW06	16.2	1.8	−3.7	4.6	92.7	7.1
VW06–VC10–VC20	20.1	3.6	1.6	2.6	120.3	6.9
G100–G200–EAST–IS12	29.5	3.6	0.3	2.0	58.4	4.0

an extension in both strain directions with only one statistically insignificant exception (Table 4). This pattern can be interpreted as an acceleration along divergent flowlines. Near Vostok Station and farther to the southeast, the divergence of the flow directions clearly dominates. For the evaluation of the standard deviations of the principal directions, the relation between major and minor principal strain rates is important. This direction becomes more uncertain if both rates have a similar magnitude (e.g. triangle 5 in the deformation network). In the case of isotropy, the strain rates are identical and the corresponding strain ellipse becomes a circle without any principal direction.

The major principal strain rates reach values up to $2{\cdot}10^{-5}$ a^{-1} which corresponds to an extension rate of 2 cm km^{-1} a^{-1}. The largest values occur in elements consisting of distant sites. However, the hypothesis of a homogeneous strain applies only approximately in these large triangles.

4.3 Transit time along the Vostok flowline

Further investigations were focused on the flowline passing through the drilling site 5G-1. The observed velocities at the sites VC10, VC20 and CNTR were orthogonally projected onto the flowline of Vostok which also runs through site G100. This mapping is based on the assumption that the velocities do not change between the observed sites and the corresponding positions on the flowline. Fig. 7 shows the velocity profile along the flowline with respect to distance (Fig. 7a) and time (Fig. 7b). Additionally, distance against time is displayed in Fig. 7(c). The velocities along the flowline upstream of the observed section were estimated by extrapolating a curve with constant acceleration fitted to the observed velocities (Fig. 7a).

The obtained trend of the velocity change along the flowline should be more realistic than the assumption of a constant flow velocity used so far. Based on this approach the transit time of the ice across the freely floating part of the lake can be calculated. The transit time for the distance of 49 km between the bedrock ridge described in Bell *et al.* (2002) and the eastern shore amounts to 28 700 years. The initial ice flow velocity at this ridge is estimated as $v_{\text{ridge}} = 1.38\,\text{m}\,\text{a}^{-1}$ assuming a constant acceleration. The uncertainties of these estimates are assessed to be in the order of 10 per cent because of the extrapolation and the assumptions made. For the entire length of the flowline on the lake (60 km), the transit-time estimate is 37 400 years which is, however, less reliable because the assumption of a constant acceleration might not apply during the grounding of the ice on the bedrock ridge. These transit times are considerably larger than earlier estimates of 16 000 years (bedrock ridge to eastern shore) and 20 000 years (shore to shore) based on a faster constant velocity (Bell *et al.* 2002).

Based on our velocity extrapolation displayed in Fig. 7 we can also estimate the transit time of an accumulation anomaly detected in ice-penetrating radar profiles (Leonard *et al.* 2004). This anomaly was deposited 26 000 years ago at the western shoreline. Our estimate of the transit time between the western shore and the present location yields 24 200 years. This indicates that the flow velocities may not have changed significantly during this period.

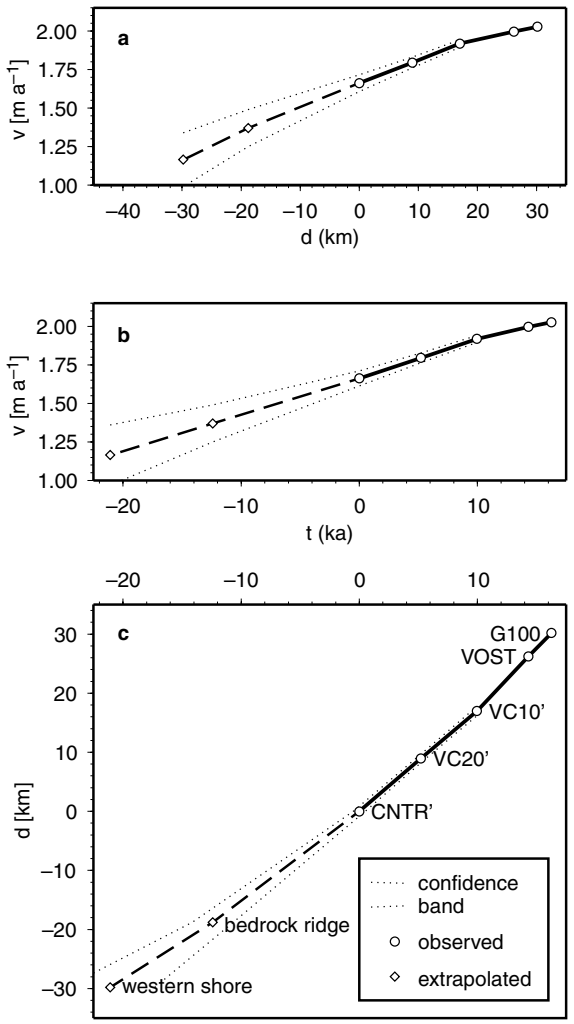

Figure 7. Empirical description of the surface kinematics along the Vostok flowline. (a) Velocity against distance along flowline, (b) velocity against time and (c) distance along the flowline against time. The points CNTR', VC20', VC10' are the projections of the corresponding GPS sites onto this flowline. Dotted lines indicate the estimated uncertainties.

With the new transit time, the thickness of the basal layer of accreted ice observed by ice-penetrating radar (Bell *et al.* 2002) can be converted into a new accretion rate estimate. For the 26 km length of the flowline between our virtual site CNTR' and Vostok Station the respective transit time is 14 300 years (Fig. 7c). Ice-penetrating radar data show a thickening of approximately 60 m of accreted ice for this specific section (Bell *et al.* 2002). With our transit time the mean accretion rate reduces to 0.004 m a^{-1} compared with the earlier estimate of 0.007 m a^{-1} (Bell *et al.* 2002).

4.4 Basal accretion rate at Vostok Station

Based on the observations obtained in the vicinity of Vostok Station, the continuity equation can be evaluated to derive independent information about the basal accretion rate at this location. This equation relates the ice thickness change with time $\partial H/\partial t$ to changes in ice flux in the north direction $\partial(uH)/\partial n$ and in the east direction $\partial(uH)/\partial e$ and to the mass balance components M and M_b (positive for mass gain expressed in mm a^{-1} ice equivalent) at the surface and the bottom respectively (Van der Veen 1999),

Table 5. Derivatives in east and north direction of ice surface h, equipotential surface N, and ice thickness H used in the continuity equation (eq. 1).

Direction	dh/dx	dN/dx	dH/dx
East	3.05×10^{-4}	5.17×10^{-5}	3.12×10^{-3}
North	6.38×10^{-4}	-1.41×10^{-5}	8.03×10^{-3}

$$\frac{\partial H}{\partial t} = -\frac{\partial(uH)}{\partial n} - \frac{\partial(vH)}{\partial e} + M + M_b. \quad (1)$$

In this equation the vertical density profile is assumed to be constant over time. Because the ice is floating across the lake without basal friction, the depth-averaged velocity components u in north direction and v in east direction are equivalent to the observed surface components. Therefore, we deduce the derivatives of the flow velocity directly from the strain parameters of the local deformation network (Table 4).

The ice thickness gradient was determined from the surface height gradient through the hydrostatic equilibrium because the measured ice thickness grid (Bell *et al.* 2002; Studinger *et al.* 2003) is too sparse for this local study. First, the height gradient components $\partial h/\partial n$ and $\partial h/\partial e$ (Table 5) were determined from the observed ellipsoidal heights h of our local network sites. As the reference surface for hydrostatic equilibrium represents an equipotential surface of the Earth's gravity field, its slope with respect to the ellipsoid has to be considered as well. This inclination is expressed by the deflection of the vertical, which is the difference between the plumb line and the ellipsoidal normal. It can be calculated as the difference between astronomically determined coordinates and the geodetic coordinates obtained by GPS. For this purpose, we performed a local GPS survey to relocate the position of the still existing site of the astronomical observations in 1963 (Liebert 1965; Leonhardt 1966) and corrected the position for the station movement from 1963 and 2003 based on the velocity for Vostok (Table 2). The resulting deflections of the vertical $\partial N/\partial n$ and $\partial N/\partial e$ are about one order of magnitude smaller than the surface gradients derived from ellipsoidal heights. The components of the ice thickness gradient $\partial H/\partial n$ and $\partial H/\partial e$ can be deduced from the surface height gradient with respect to the equipotential surface according to the hydrostatic equilibrium

$$\frac{\partial H}{\partial x} = \left(1 - \frac{\rho_{\text{ice}}}{\rho}\right)^{-1} \cdot \left(\frac{\partial h}{\partial x} - \frac{\partial N}{\partial x}\right). \quad (2)$$

The conversion factor (first term of eq. 2) was derived from the grid of measured ice thicknesses mentioned above and corresponding surface elevations to be 12.3 for the southern part of the lake. The components of the resulting ice thickness gradient are listed in Table 5.

Returning to eq. (1) the surface mass balance M is 0.024 m a^{-1} $\pm$ 0.004 m a^{-1} ice equivalent according to Barkov & Lipenkov (1996).

Under the assumption of steady state ($\partial H/\partial t = 0$), the local accretion rate is 0.016 m a^{-1}. From error propagation of eq. (1) we derive a standard deviation of 0.006 m a^{-1}.

If we introduce the estimated accretion rate of 0.004 m a^{-1} from Section 4.3 the resulting ice thickness change is -0.012 m a^{-1} $\pm$ 0.006 m a^{-1}. Hence, the validity of the steady state hypothesis has a large influence on the calculated accretion rate.

5 CONCLUSIONS

We used GPS observations acquired during two field seasons to derive ice flow velocities at 10 sites in the vicinity of Vostok Station.

The surface velocity at Vostok Station was determined to be $2.00\,\mathrm{m\,a^{-1}} \pm 0.01\,\mathrm{m\,a^{-1}}$ at an azimuth of $133.7^\circ \pm 0.3^\circ$ relative to true north. This rate is up to 50 per cent smaller than previous estimates. Additionally, there is clear evidence for an acceleration along the flowlines of the ice sheet traversing the lake from the western to the southeastern shore, with a longitudinal strain rate on the order of $10^{-5}\,\mathrm{a^{-1}}$. The velocity along the flow trajectory through the drilling site 5G-1 increases from extrapolated $1.38\,\mathrm{m\,a^{-1}} \pm 0.15\,\mathrm{m\,a^{-1}}$ at the bedrock ridge where the ice is grounded in the west, up to measured $2.03 \pm 0.01\,\mathrm{m\,a^{-1}}$ at the southeastern shoreline. The flow directions at all GPS sites on the lake are parallel to the trajectories derived from structure tracking (Bell *et al.* 2002; Tikku *et al.* 2004). Our estimation of the traveltime of an accumulation anomaly deposited at the western shore 26 000 years ago (Leonard *et al.* 2004) using the present-day flow velocities yields 24 200 years. Both aspects may indicate stable ice flow during the last 20 000 years at least.

A strain analysis used to describe the horizontal deformation field in the vicinity of Vostok Station yields a horizontal major principal strain rate of 1–2 $\mathrm{cm\,km^{-1}\,yr^{-1}}$ as well as divergent ice flow. The ice flow along the Vostok flowline can be parametrized by a constant acceleration. This approach leads to longer transit times across the lake than previously estimated. For the section from the bedrock ridge northwest of Vostok Station to the eastern shoreline the transit time is 28 700 years.

Based on the measured thickness of the accreted ice layer (Bell *et al.* 2002) and our velocities, the mean accretion rate for a 26 km portion of the flowline upstream of Vostok Station is estimated to be $0.004\,\mathrm{m\,a^{-1}}$.

Independently, the basal accretion at Vostok Station can also be derived from an evaluation of the continuity equation using the observed geodetic quantities. If we assume steady state, the basal accretion rate is $0.016\,\mathrm{m\,a^{-1}}$. On the contrary, the above-estimated accretion rate of $0.004\,\mathrm{m\,a^{-1}}$ results in an ice thickness change at Vostok of $-0.012\,\mathrm{m\,a^{-1}}$. The observed vertical ice-particle velocity of $0.07\,\mathrm{m\,a^{-1}}$ for Vostok Station is—neglecting minor contributions of surface slope and isostatic effect—largely compensated by the mean snow accumulation of $0.06\,\mathrm{m\,a^{-1}}$. Thus, we see no indication of a surface height change caused either by an ice mass imbalance or by a change in the lake level during the time covered by the observations.

ACKNOWLEDGMENTS

This work was supported by the German Research Foundation (Deutsche Forschungsgemeinschaft) and by the Heiwa-Nakajima Zaidan Fund, Japan. We would like to acknowledge the logistical assistance of the Russian team at Vostok Station during both field seasons.

The conversion factor for the hydrostatic equilibrium calculation (eq. 2 in Section 4.4) was derived using the ice thickness data acquired in the frame of a National Science Foundation project (Grant OPP-9911617) (Studinger *et al.* 2003). We thank Robin Bell and one anonymous reviewer for their helpful comments.

REFERENCES

Altamimi, Z., Sillard, P. & Boucher, C., 2002. ITRF2000: A new release of the International Terrestrial Reference Frame for earth science applications, *J. geophys. Res.,* **107**(B10), 2214, doi:10.1029/2001JB000561.

Barkov, N.I. & Lipenkov, V.Y., 1996. Snow accumulation at Vostok Station, Antarctica, in 1970–1992, *Materialy Glyatsiologicheskikh Issledovanii,* **80,** 87–88.

Bell, R.E., Studinger, M., Tikku, A.A., Clarke, G.K.C., Gutner, M.M. & Meertens, C., 2002. Origin and fate of Lake Vostok water frozen to the base of the East Antarctic ice sheet, *Nature,* **416,** 307–310.

Boucher, C., Altamimi, Z., Sillard, P. & Feissel-Vernier, M., 2004. *The ITRF2000,* no. 31 in IERS Technical Note, IERS ITRS Centre, Verlag des Bundesamts für Kartographie und Geodāsie, Frankfurt-on-Main.

Bulat, S.A. *et al.*, 2004. DNA signature of thermophilic bacteria from the aged accretion ice of Lake Vostok, Antarctica: implications for searching for life in extreme icy environments, *International Journal of Astrobiology,* **3**(1), 1–12, doi:10.1017/S1473550404001879.

Dietrich, R., Rülke, A., Ihde, J., Lindner, K., Miller, H., Niemeier, W., Schenke, H.-W. & Seeber, G., 2004. Plate kinematics and deformation status of the Antarctic Peninsula based on GPS, *Global and Planetary Change,* **42,** 313–321.

Hooke, R.L., 1998. *Principles of Glacier Mechanics*, Prentice Hall, Upper Saddle River, New Jersey.

Hugentobler, U., Dach, R. & Fridez, P., 2004. *Bernese GPS Software Version 5.0—Draft,* Astronomical Institute, University of Berne, Berne, Switzerland.

IGb00, 2004. igscb.jpl.nasa.gov/network/refframe.html.

Jezek, K. & RAMP Product Team, 2002. RAMP AMM-1 SAR Image Mosaic of Antarctica, Fairbanks, AK: Alaska SAR Facility, in association with the National Snow and Ice Data Center, Digital media. Boulder, Colorado.

Kapitsa, A.P., Ridley, J.K., Robin, G. de Q., Siegert, M.J. & Zotikov, I.A., 1996. A large deep freshwater lake beneath the ice of central East Antarctica, *Nature,* **381,** 684–686.

Karl, D.M., Bird, D.F., Björkman, K., Houlihan, T., Shackelford, R. & Tupas, L., 1999. Microorganisms in the Accreted Ice of Lake Vostok, Antarctica, *Science,* **286,** 2144–2147.

Kwok, R., Siegert, M.J. & Carsey, F.D., 2000. Ice motion over Lake Vostok, Antarctica: constraints on inferences regarding the accreted ice, *Journal of Glaciology,* **46**(155), 689–694.

Leonard, K., Bell, R.E., Studinger, M. & Tremblay, B., 2004. Anomalous accumulation rates in the Vostok ice-core resulting from ice flow over Lake Vostok, *Geophys. Res. Lett.,* **31,** L24401, doi:10.1029/2004GL021102.

Leonhardt, G., 1966. Meßmethodik und Ergebnisse astronomischer Ortsbestimmungen in der Antarktis, *Geodätische und geophysikalische Veröffentlichungen,* **Reihe I**(2), 44–47.

Liebert, J., 1965. Astronomische Ortsbestimmung in der Antarktis, *Vermessungstechnik,* **13**(9), 325–327.

Liebert, J. & Leonhardt, G., 1973. Astronomic observations for determining ice movement in the Vostok Station area, *Sov. Antarct. Exped. Inf. Bull.,* **88,** 68–70.

Masolov, V.N., Lukin, V.V., Sheremetiev, A.N. & Popov, S.V., 2001. Geophysical Investigations of the Subglacial Lake Vostok in Eastern Antarctica, *Doklady Earth Sciences,* **379A**(6), 734–738.

Mayer, C. & Siegert, M.J., 2000. Numerical modelling of ice-sheet dynamics across the Vostok subglacial lake, central East Antarctica, *Journal of Glaciology,* **46**(153), 197–205.

Parrenin, F., Rémy, F., Ritz, C., Siegert, M.J. & Jouzel, J., 2004. New modeling of the Vostok ice flow line and implication for the glaciological chronology of the Vostok ice core, *J. geophys. Res.,* **109,** D20102, doi:10.1029/2004JD004561.

Pattyn, F., De Smedt, B. & Souchez, R., 2004. Influence of subglacial Lake Vostok on the regional ice dynamics of the Antarctic ice sheet: a model study, *accepted for Journal of Glaciology* **50,** 583–589.

Petit, J.R. *et al.*, 1999. Climate and atmospheric history of the past 420,000 years from the Vostok ice core, Antarctica, *Nature,* **399,** 429–436.

Priscu, J.C. *et al.*, 1999. Geomicrobiology of Subglacial Ice Above Lake Vostok, Antarctica, *Science,* **286,** 2141–2144.

Ray, J., Dong, D. & Altamimi, Z., 2004. IGS reference frames: status and future improvements, *GPS Solutions,* **8**(4), 251–266, doi:10.1007/s10291–004–0110–x.

Rémy, F., Shaeffer, P. & Legrésy, B., 1999. Ice flow physical processes derived from ERS-1 high-resolution map of the Antarctica and Greenland ice sheets, *Geophys. J. Int.,* **139,** 645–656.

Siegert, M.J. & Bamber, J.L., 2000. Subglacial water at the heads of Antarctic ice-stream tributaries, *Journal of Glaciology,* **46**(155), 702–703.

Siegert, M.J., Carter, S., Tabacco, I., Popov, S. & Blankenship, D.D., 2005. A revised inventory of Antarctic subglacial lakes, *Antarctic Science,* **17**(3), 453–460, doi:10.1017/S0954102005002889.

Studinger, M. *et al.*, 2003. Ice cover, landscape setting, and geological framework of Lake Vostok, East Antarctica, *Earth planet. Sci. Lett.,* **205**(3–4), 195–210.

Tikku, A.A., Bell, R.E., Studinger, M. & Clarke, G.K.C., 2004. Ice flow field over Lake Vostok, East Antarctica inferred by structure tracking, *Earth planet. Sci. Lett.,* **227,** 249–261, doi:10.1016/j.epsl.2004.09.021.

Van der Veen, C.J., 1999. *Fundamentals of Glacier Dynamics,* A.A. Balkema, Rotterdam, Brookfield.

Wendt, A. *et al.*, 2005. The response of the subglacial Lake Vostok, Antarctica, to tidal and atmospheric pressure forcing, *Geophys. J. Int.,* **161,** 41–49, doi:10.1111/j.1365–246X.2005.02575.x.

Wingham, D.J., Siegert, M.J., Shepherd, A. & Muir, A.S., 2006. Rapid discharge connects Antarctic subglacial lakes, *Nature,* **440,** 1033–1036, doi:10.1038/nature04660.